CHEMMEDCHEM
Chemistry & Drug Discovery

Supporting Information

Discovery and Mechanistic Elucidation of a Class of Protein Disulfide Isomerase Inhibitors for the Treatment of Glioblastoma

Anahita Kyani[+],[a] Shuzo Tamura[+],[a] Suhui Yang[+],[a] Andrea Shergalis[+],[a] Soma Samanta,[a] Yuting Kuang,[a] Mats Ljungman,[b] and Nouri Neamati*[a]

cmdc_201700629_sm_miscellaneous_information.pdf

Author Contributions

A.K. Data curation: Lead; Formal analysis: Lead; Investigation: Equal; Writing – original draft: Lead; Writing – review & editing: Equal
S.T. Data curation: Equal; Formal analysis: Equal; Writing – review & editing: Equal
S.Y. Data curation: Equal; Formal analysis: Equal; Writing – original draft: Supporting; Writing – review & editing: Equal
A.S. Data curation: Equal; Formal analysis: Supporting; Writing – review & editing: Equal
S.S. Data curation: Supporting; Writing – review & editing: Supporting
Y.K. Data curation: Supporting; Writing – review & editing: Supporting
M.L. Conceptualization: Supporting; Formal analysis: Supporting; Project administration: Supporting; Resources: Equal; Supervision: Supporting; Writing – review & editing: Supporting
N.N. Conceptualization: Lead; Data curation: Lead; Funding acquisition: Lead; Project administration: Lead; Resources: Lead; Supervision: Lead; Writing – review & editing: Supporting.

Table of Contents

Table S1. 35G8 analogues available from the NCI database. Compounds marked with an asterisk (*) were ordered from the NCI.

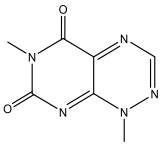

67078*

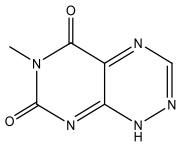

99733*

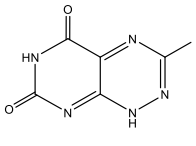

104989*

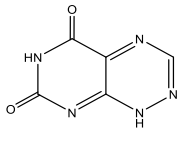

114402

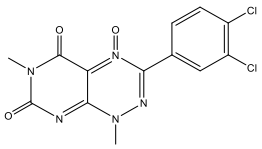

277834

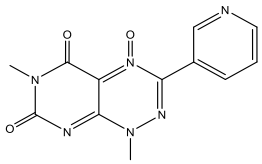

277835

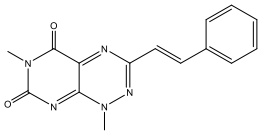

277836

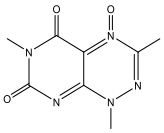

280172*

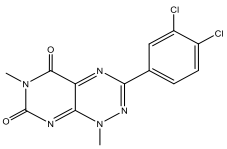

280173*

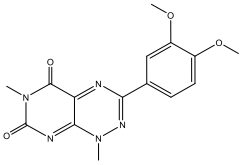

280174*

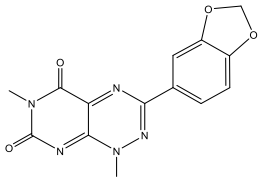

280175

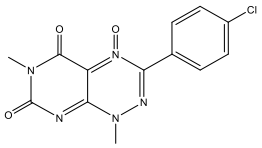

280176*

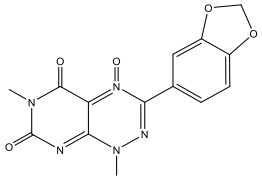

280177*

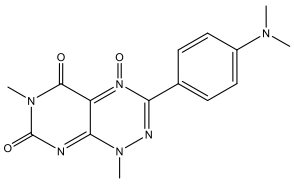

280178

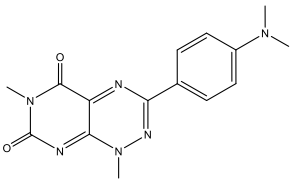

280308

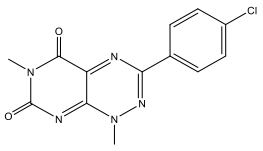

749675

A

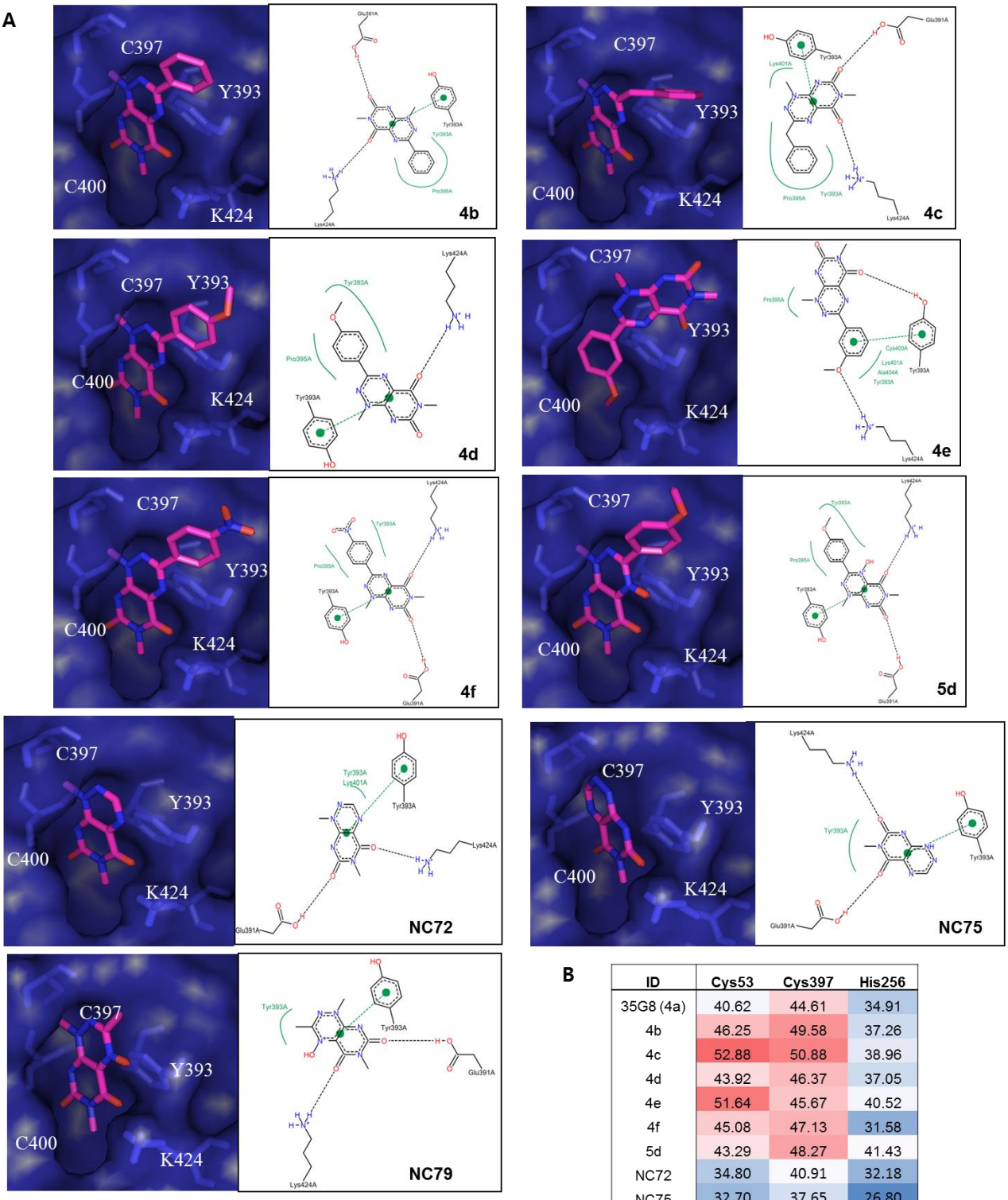

B

ID	Cys53	Cys397	His256
35G8 (4a)	40.62	44.61	34.91
4b	46.25	49.58	37.26
4c	52.88	50.88	38.96
4d	43.92	46.37	37.05
4e	51.64	45.67	40.52
4f	45.08	47.13	31.58
5d	43.29	48.27	41.43
NC72	34.80	40.91	32.18
NC75	32.70	37.65	26.80
NC79	37.06	43.96	36.44

Figure S1. Docking poses of **35G8** analogues. (A) Docking poses of the **35G8** analogues docked in the Cys397 catalytic site of PDI along with PoseView representation showing the interactions with the binding site residues. (B) Heat map plot for docking of **35G8** analogues toward three binding sites of PDI.

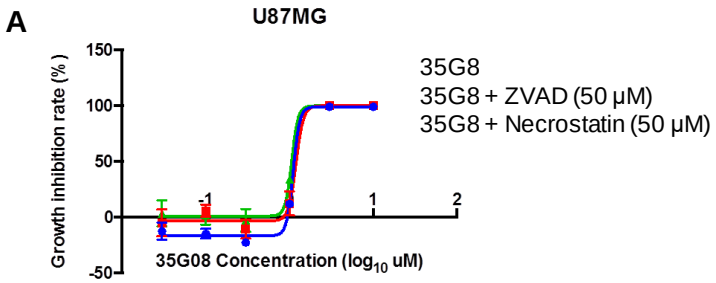

IC_{50} (µM)		
35G8	**35G8+ZVAD**	**35G8+Necrostatin**
1.12 ± 0.04	1.22 ± 0.11	1.06 ± 0.01

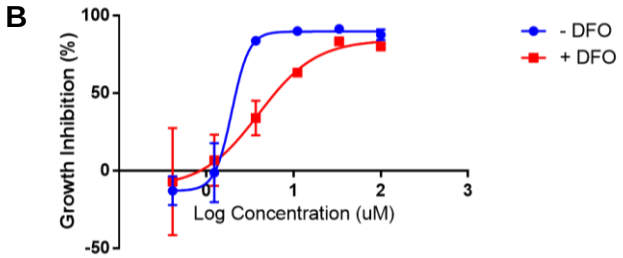

Figure S2. (A) Cytotoxicity data for U87MG cells treated with Z-VAD-FMK (50 µM) or necrostatin (50 µM) + **35G8**. (B) DFO decreases the potency of **35G8**. U87MG cells were subjected to 100 µM DFO at increasing concentrations of **35G8**. Results are means from three independent experiments; error bars show s.d.

Table S2. Top 20 upregulated genes upon **35G8** treatment

Gene Symbol	Gene Name (Description)	Fold change
SLC7A11	solute carrier family 7, (cationic amino acid transporter, y+ system) member 11	62.28
AKR1C1	interleukin-6 (IL-6), aldo-keto reductase 1C1	59.25
CHAC1	ChaC, cation transport regulator homolog 1 (E. coli)	46.09
TMEM74	transmembrane protein 74	27.77
LOC344887	similar to hCG2041270	23.27
TRIB3	tribbles homolog 3 (Drosophila)	23.22
LOC388692	similar to UPF0627 protein ENSP00000358171; hypothetical LOC388692	19.60
HMOX1	heme oxygenase (decycling) 1	19.16
F2RL2	coagulation factor II (thrombin) receptor-like 2	17.42
WDR74	WD repeat domain 74	17.31
TNFSF9	tumor necrosis factor (ligand) superfamily, member 9	17.05
TMEM107	transmembrane protein 107	15.22
C12orf57	chromosome 12 open reading frame 57	14.33
LOC643723	hypothetical LOC643723	13.44
INHBA	inhibin, beta A	13.14
ARG2	arginase, type II	12.46
IRS2	insulin receptor substrate 2	11.73
HKDC1	hexokinase domain containing 1	11.41
GLA	galactosidase, alpha	11.26
BTG2	BTG family, member 2	10.98

Table S3. Top 20 downregulated genes upon **35G8** treatment

Gene Symbol	Gene Name (Description)	Fold change
TXNIP	thioredoxin interacting protein	-7.40
EGR1	early growth response 1	-5.65
HIST1H2AB	histone cluster 1, H2ae; histone cluster 1, H2ab	-5.08
CSF3	colony stimulating factor 3 (granulocyte)	-4.96
HIST1H2AC	histone cluster 1, H2ac	-4.52
HIST1H2BO	histone cluster 1, H2bo	-4.40
HIST1H2BK	histone cluster 1, H2bk	-4.37
HIST1H2BJ	histone cluster 1, H2bj	-4.37
STAMBPL1	STAM binding protein-like 1	-4.35
PRDM8	PR domain containing 8	-4.28
HIST1H2BE	histone cluster 1, H2be	-4.23
HIST1H2AL	histone cluster 1, H2al	-4.21
MIF	macrophage migration inhibitory factor (glycosylation-inhibiting factor)	-4.06
HIST1H3G	histone cluster 1, H3g	-3.99
NDP	Norrie disease (pseudoglioma)	-3.99
POLR2L	polymerase (RNA) II (DNA directed) polypeptide L, 7.6kDa	-3.98
ITGA3	integrin, alpha 3 (antigen CD49C, alpha 3 subunit of VLA-3 receptor)	-3.89
HIST1H3D	histone cluster 2, H3d	-3.89
HIST1H3F	histone cluster 1, H3f	-3.84
ID1	inhibitor of DNA binding 1, dominant negative helix-loop-helix protein	-3.80

Table S4. Top 20 Ingenuity canonical pathways correlating with **35G8** treatment identified by IPA

Ingenuity Canonical Pathway	p-value	Molecules
NRF2-mediated Oxidative Stress Response	6.03E-10	PPIB, PRDX1,NQO2,ABCC2,DNAJC6,HSPB8,GCLC,HMOX1,KEAP1, JUND, TXN,DNAJB1,GCLM,MGST1,NQO1, HERPUD1,DNAJB9, TXNRD1,GSR, FOS,DNAJB11,SQSTM1, ENC1,FTH1,EPHX1
Unfolded protein response	9.55E-08	SEL1L,CALR,HSP90B1,UBXN4,DDIT3,HSPA9, XBP1,CANX,CEBPB,DNAJB9,HSPA5,CEBPG
tRNA Charging	2.63E-06	CARS,WARS,YARS,GARS,AARS,SARS,MARS, IARS,EPRS
Aryl Hydrocarbon Receptor Signaling	3.24E-05	HSPB3,MGST1,IL1A,NQO2,NQO1,MDM2,BAX, CCND1, FOS,HSP90B1,NCOA7,ALDH1L2,AHR,CDK2,HSPB1
Protein Ubiquitination Pathway	8.71E-05	HSPB3,CDC20,DNAJC6,HSPA9,HSPB8,MDM2, PSMB8,HSPA5,SKP1,DNAJB9,UBE2D1,UCHL1,PAN2,HSP90B1,UBE2H,DNAJB11,HSPA13,PSMA3,DNAJB1,UBC,HSPB1
IL-6 Signaling	9.77E-05	HSPB3,IL6ST,CXCL8,IL1A,IL6R,CEBPB,IL36B, VEGFA,COL1A1,FOS,IKBKG,IL36RN,HSPB1
Antigen Presentation Pathway	1.58E-04	CALR,PDIA3,HLA-DMA,HLA-DRA,CIITA,CANX,PSMB8
Aldosterone Signaling in Epithelial Cells	4.07E-04	HSPB3,PDIA3,DNAJC6,HSPA9,HSPB8,ITPR1, DNAJB9,HSPA5,SLC9A1,HSP90B1,DNAJB11, HSPA13,DNAJB1,HSPB1
Endoplasmic Reticulum Stress Pathway	4.68E-04	CALR,HSP90B1,DDIT3,XBP1,HSPA5
Vitamin-C Transport	8.51E-04	TXN,GLRX,SLC2A3,TXNRD1
Superpathway of Serine and Glycine Biosynthesis I	1.07E-03	PSAT1,PHGDH,SHMT2
Role of Macrophages, Fibroblasts and Endothelial Cells in Rheumatoid Arthritis	2.69E-03	IL6ST,CXCL8,MIF,IL1A,MMP3,PDIA3,FGF2,DAAM1, IL6R,CEBPB,CREB5, CCND1,CEBPG,IL36B,VEGFA, FOS,IKBKG,IL36RN,NFATC2
Glutathione Biosynthesis	3.09E-03	GCLC,GCLM
Glutathione Redox Reactions II	3.09E-03	GSR,GLRX
Methylglyoxal Degradation III	3.39E-03	AKR1C1/AKR1C2,AKR1B1,AKR1B10
Mitotic Roles of Polo-Like Kinase	4.17E-03	CDC25C,HSP90B1,PLK4,CDC20,PLK2,WEE1,PLK1
Hypoxia Signaling in the Cardiovascular System	4.17E-03	VEGFA,HSP90B1,UBE2H,NQO1,MDM2,CREB5, UBE2D1
p53 Signaling	4.47E-03	PMAIP1,TP53INP1,GADD45A,MDM2,BAX,PML, CCND1,CDK2,SERPINE2
p38 MAPK Signaling	4.68E-03	HSPB3,TGFBR2,IL1A,DDIT3,DUSP10,HIST1H3C, IL36RN,CREB5,IL36B,HSPB1
Cell Cycle: G2/M DNA Damage Checkpoint Regulation	4.79E-03	CDC25C,GADD45A,WEE1,MDM2,PLK1,SKP1

Table S5. Top 20 gene sets for upregulated genes from **35G8** treatment obtained by GSEA

Gene set	Size	NES	FDR q-val
NFE2L2.V2	154	2.702	< E-06
PODAR_RESPONSE_TO_ADAPHOSTIN_UP	115	2.665	< E-06
GSE9988_ANTI_TREM1_AND_LPS_VS_VEHICLE_TREATED_ MONOCYTES_UP	127	2.664	< E-06
GARGALOVIC_RESPONSE_TO_OXIDIZED_PHOSPHOLIPIDS_ BLUE_UP	113	2.629	< E-06
BLUM_RESPONSE_TO_SALIRASIB_UP	201	2.558	< E-06
GSE9988_ANTI_TREM1_VS_CTRL_TREATED_MONOCYTES_UP	143	2.550	< E-06
HELLER_SILENCED_BY_METHYLATION_DN	62	2.515	< E-06
GSE9988_ANTI_TREM1_VS_VEHICLE_TREATED_MONOCYTES_ UP	135	2.510	< E-06
TIEN_INTESTINE_PROBIOTICS_24HR_DN	181	2.498	< E-06
KRIGE_AMINO_ACID_DEPRIVATION	25	2.486	< E-06
GHANDHI_BYSTANDER_IRRADIATION_UP	47	2.438	< E-06
GSE9988_ANTI_TREM1_AND_LPS_VS_CTRL_TREATED_ MONOCYTES_UP	138	2.438	< E-06
MTOR_UP.N4.V1_UP	121	2.433	< E-06
CONCANNON_APOPTOSIS_BY_EPOXOMICIN_UP	159	2.428	< E-06
PACHER_TARGETS_OF_IGF1_AND_IGF2_UP	20	2.414	< E-06
ONDER_CDH1_TARGETS_2_DN	109	2.354	< E-06
GSE22886_DAY0_VS_DAY1_MONOCYTE_IN_CULTURE_DN	131	2.345	< E-06
ONDER_CDH1_TARGETS_1_UP	65	2.344	< E-06
GHANDHI_DIRECT_IRRADIATION_UP	59	2.343	< E-06
GERY_CEBP_TARGETS	63	2.329	< E-06

Table S6. Top 20 gene sets for downregulated genes from **35G8** treatment obtained by GSEA

Gene set	**Size**	**NES**	**FDR q-val**
GNF2_CENPF	59	-2.842	< E-06
GNF2_CCNA2	66	-2.801	< E-06
ROSTY_CERVICAL_CANCER_PROLIFERATION_CLUSTER	122	-2.792	< E-06
GNF2_CCNB2	52	-2.726	< E-06
ZHOU_CELL_CYCLE_GENES_IN_IR_RESPONSE_24HR	108	-2.709	< E-06
GNF2_PCNA	66	-2.698	< E-06
KOBAYASHI_EGFR_SIGNALING_24HR_DN	226	-2.666	< E-06
GNF2_CDC2	59	-2.659	< E-06
GNF2_CDC20	52	-2.640	< E-06
ZHOU_CELL_CYCLE_GENES_IN_IR_RESPONSE_6HR	74	-2.637	< E-06
GNF2_SMC4L1	83	-2.613	< E-06
CHANG_CYCLING_GENES	123	-2.595	< E-06
GNF2_HMMR	46	-2.587	< E-06
ISHIDA_E2F_TARGETS	45	-2.584	< E-06
GNF2_RRM2	38	-2.572	< E-06
GNF2_FEN1	56	-2.547	< E-06
GNF2_MCM4	52	-2.507	< E-06
CROONQUIST_NRAS_SIGNALING_DN	61	-2.507	< E-06
GNF2_MKI67	27	-2.491	< E-06

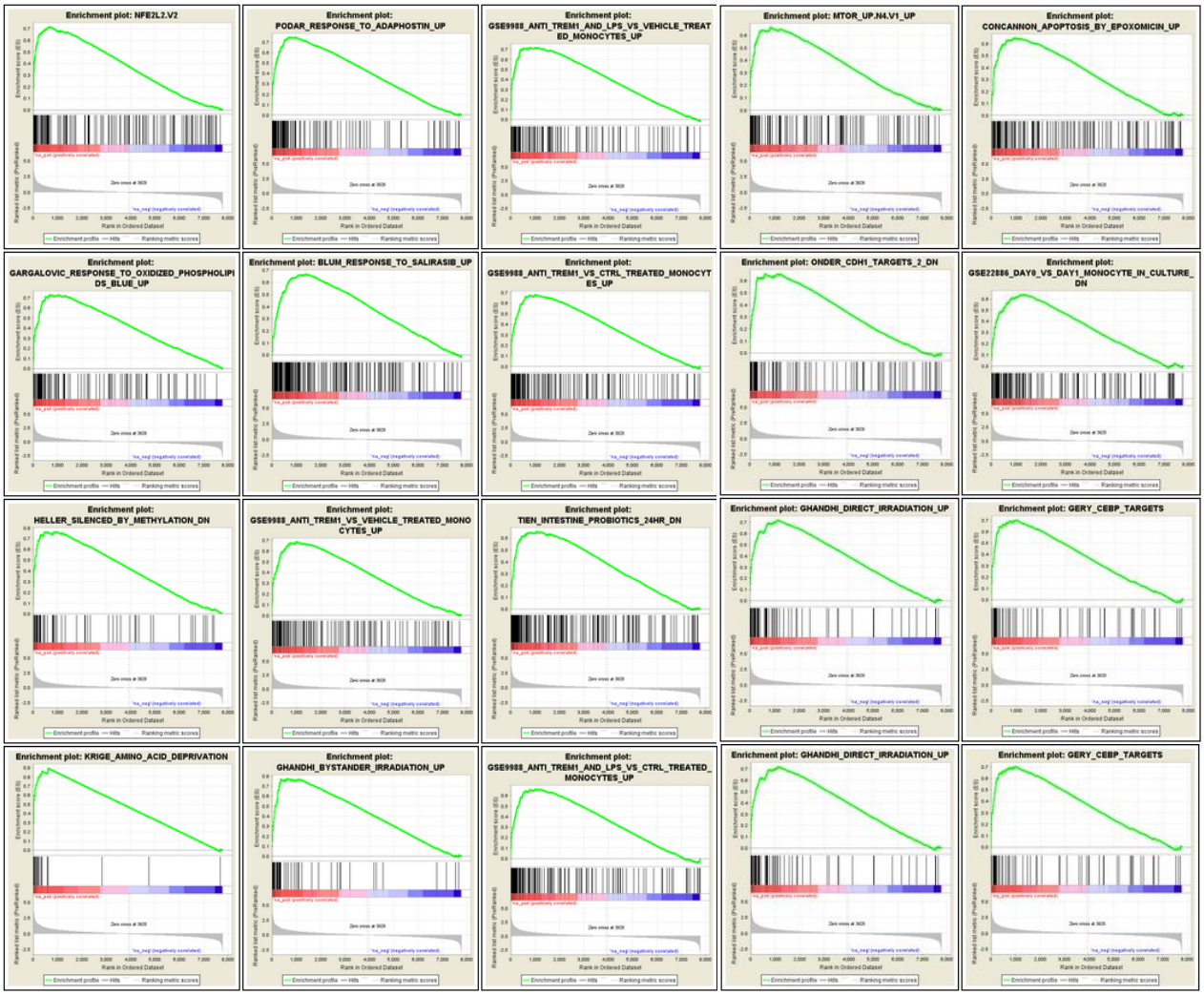

Figure S3. GSEA snapshots of enriched gene sets for genes upregulated by **35G8** treatment from Bru-Seq results.

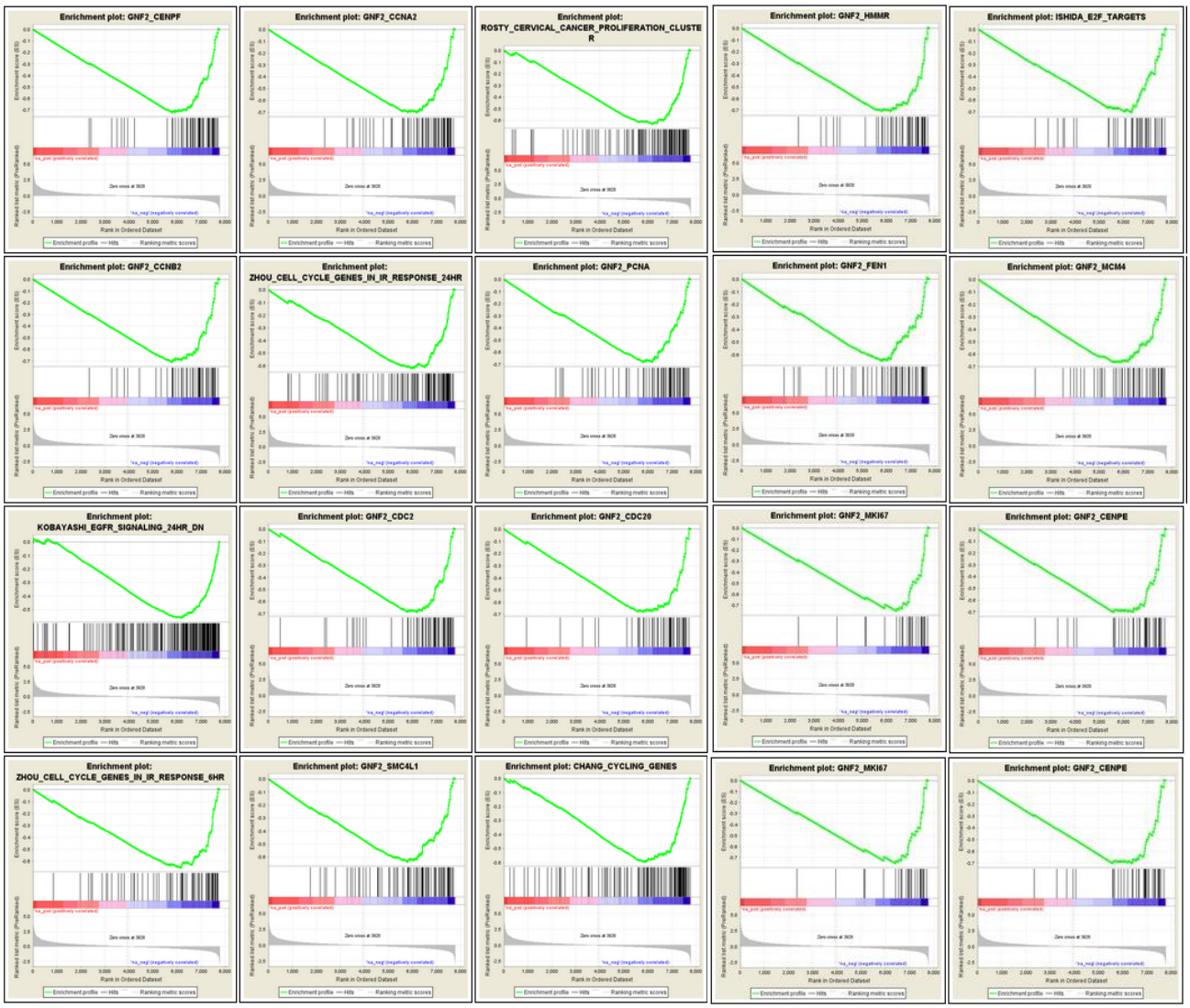

Figure S4. GSEA snapshots of enriched gene sets for genes downregulated by **35G8** based on Bru-Seq results.

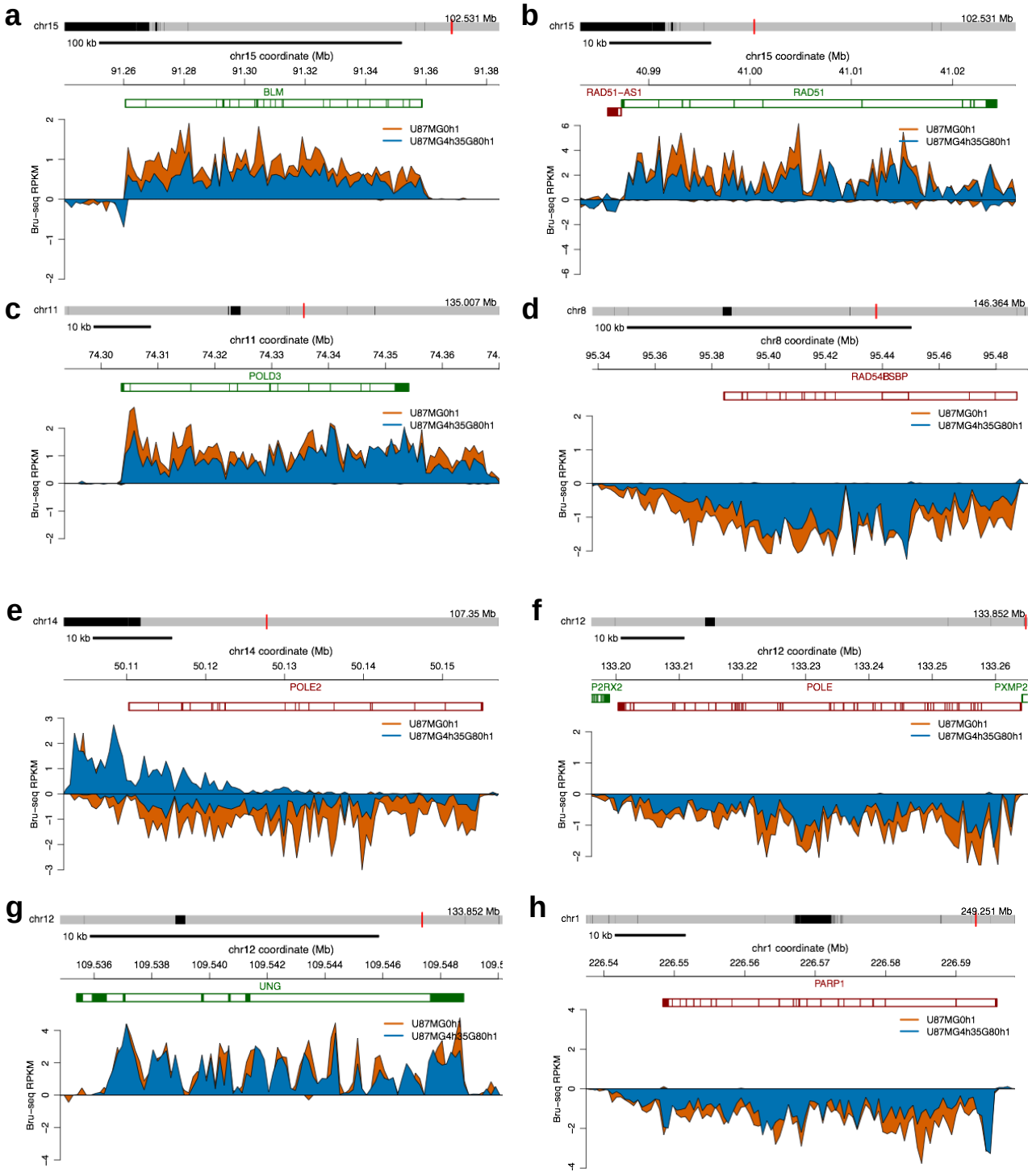
a
chr15
102.531 Mb
100 kb
chr15 coordinate (Mb)
91.26 91.28 91.30 91.32 91.34 91.36 91.38
BLM
U87MG0h1
U87MG4h35G80h1
Bru−seq RPKM
b
chr15
102.531 Mb
10 kb
chr15 coordinate (Mb)
40.99 41.00 41.01 41.02
RAD51−AS1
RAD51
U87MG0h1
U87MG4h35G80h1
Bru−seq RPKM
c
chr11
135.007 Mb
10 kb
chr11 coordinate (Mb)
74.30 74.31 74.32 74.33 74.34 74.35 74.36
POLD3
U87MG0h1
U87MG4h35G80h1
Bru−seq RPKM
d
chr8
146.364 Mb
100 kb
chr8 coordinate (Mb)
95.34 95.36 95.38 95.40 95.42 95.44 95.46 95.48
RAD54BSBP
U87MG0h1
U87MG4h35G80h1
Bru−seq RPKM
e
chr14
107.35 Mb
10 kb
chr14 coordinate (Mb)
50.11 50.12 50.13 50.14 50.15
POLE2
U87MG0h1
U87MG4h35G80h1
Bru−seq RPKM
f
chr12
133.852 Mb
10 kb
chr12 coordinate (Mb)
133.20 133.21 133.22 133.23 133.24 133.25 133.26
P2RX2
POLE
PXMP2
U87MG0h1
U87MG4h35G80h1
Bru−seq RPKM
g
chr12
133.852 Mb
10 kb
chr12 coordinate (Mb)
109.536 109.538 109.540 109.542 109.544 109.546 109.548
UNG
U87MG0h1
U87MG4h35G80h1
Bru−seq RPKM
h
chr1
249.251 Mb
10 kb
chr1 coordinate (Mb)
226.54 226.55 226.56 226.57 226.58 226.59
PARP1
U87MG0h1
U87MG4h35G80h1
Bru−seq RPKM

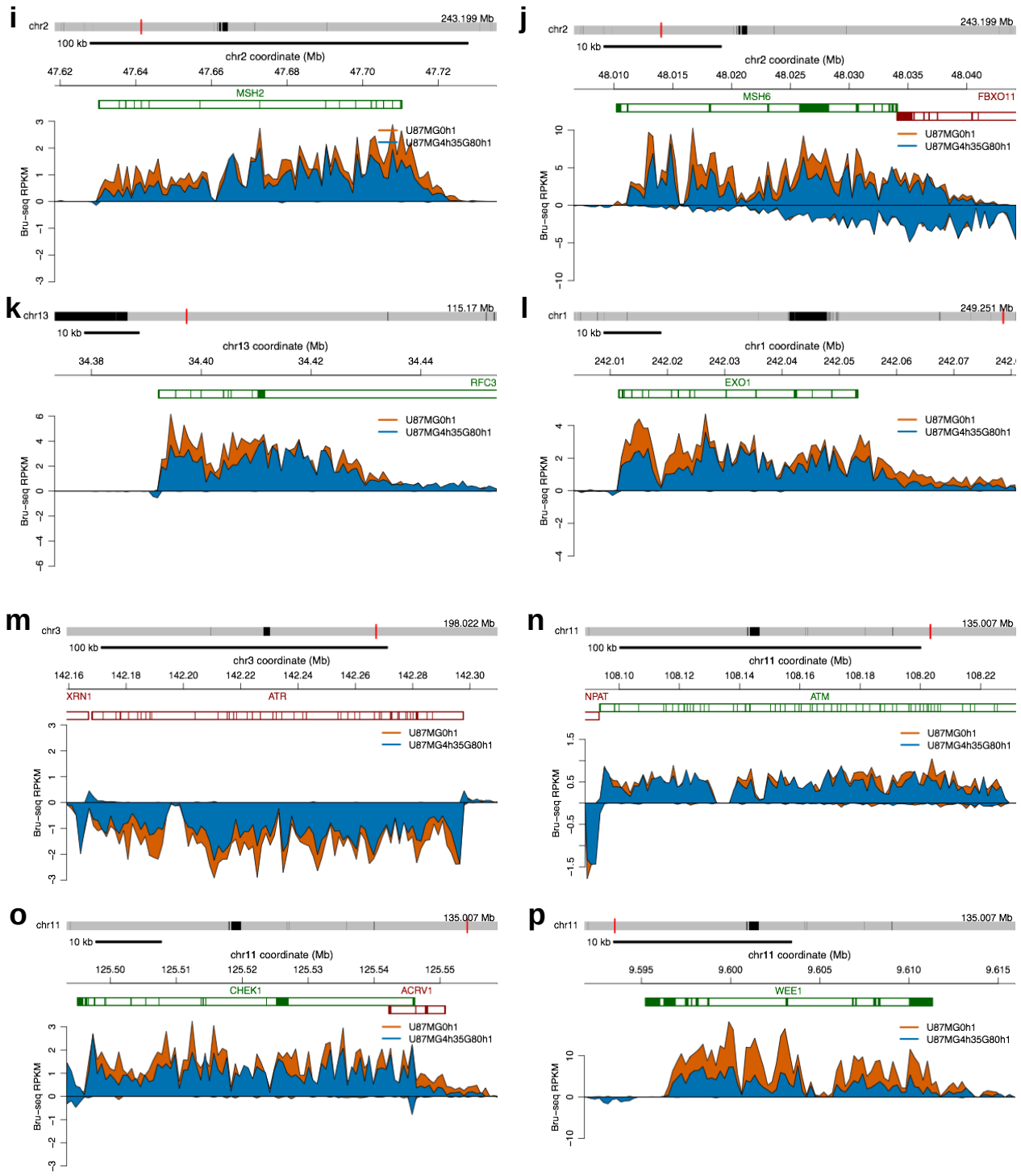

Figure S5. 35G8 treatment decreases the rate of transcription of several genes involved in DNA repair pathways including (a) *blm*, (b) *rad51*, (c) *pold3*, (d) *rad54fbsbp*, (e) *pole2*, (f) *pole*, (g) *ung*, (h) *parp1*, (i) *msh2*, (j) *msh6*, (k) *rfc3*, (l) *exo1*, (m) *atr*, (n) *atm*, (o) *chek1*, and (p) *wee1*.

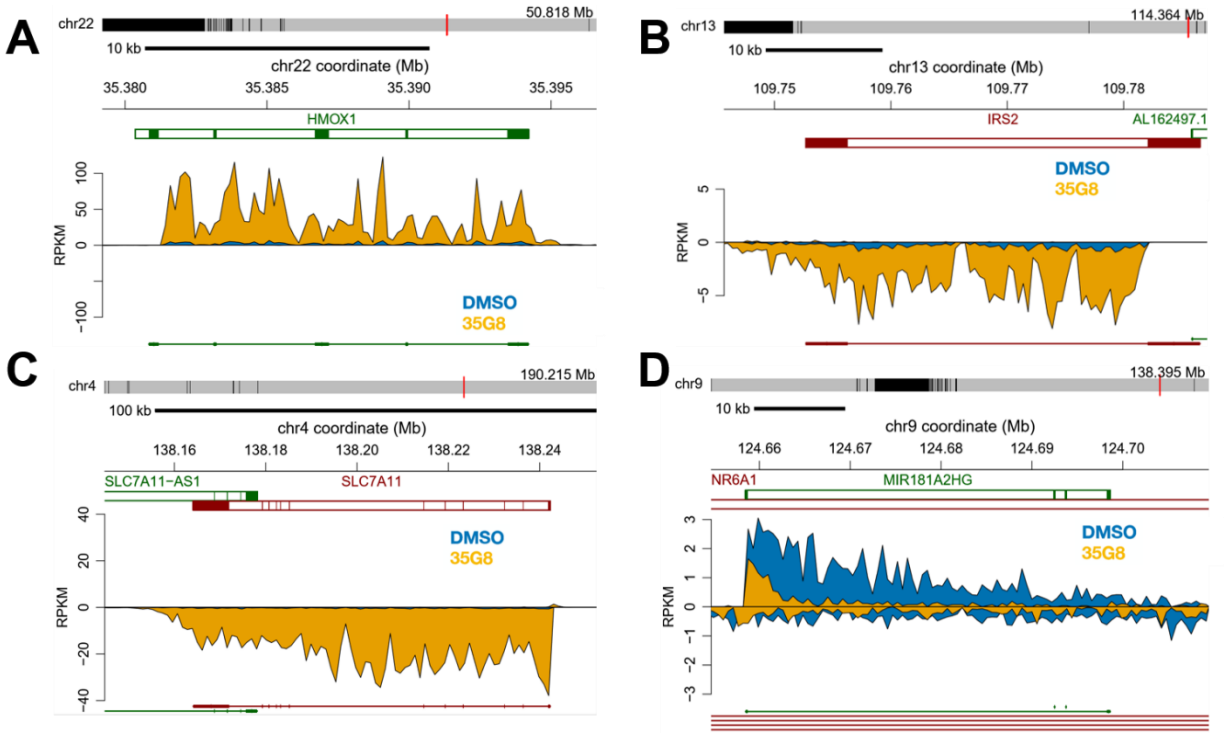

Figure S6. 35G8 treatment increases the rate of transcription of (a) *hmox1*, (b) *irs2*, and (c) *slc7a11* and decreases the rate of transcription of (d) *mir181A2HG*.

Table S7. IC_{50} values for **35G8** + NAC treatment in glioblastoma cancer cell lines. Four concentrations of NAC added to cells with **35G8**.

Cell Lines	**35G8** IC_{50} (μM) +**NAC (mM)**				IC_{50} (mM) **NAC only**
	0	**1**	**5**	**10**	
U87MG	1.1 ± 0.02	1.1	1.2	0.8	10.0
U118MG	2.0 ± 0.6	0.7	0.6	0.03	10.1
NU04	0.8 ± 0.2	0.8	0.9	0.8	10.5
A172	3.9 ± 0.1	1.6	1.8	1.5	10.6

Table S8. Chemical properties of synthesized **35G8** analogues

Molecule	**MW**	**ALogP**	**S+Sw**[a]	**T_PSA**[b]	**NRBO**[c]	**S+BBB_Filter**[d]
35G8 (4a)	207.19	-1.08	5.34	82.7	0	High
4b	269.26	0.59	0.38	82.7	1	High
4c	283.29	0.62	0.76	82.7	2	High
4d	299.28	0.57	0.38	91.9	2	High
4f	314.26	0.48	0.29	128.0	2	High
5d	315.28	0.29	5.18	104.0	2	High

[a] Water solubility (mg/ml) calculated by ADMET predictor
[b] Topological version of polar surface area calculated by ADMET predictor
[c] Number of rotatable bonds
[d] Likelihood of blood brain barrier penetration. Classification confidence: High = 97%, Low = 84%. Overall accuracy = 94%.

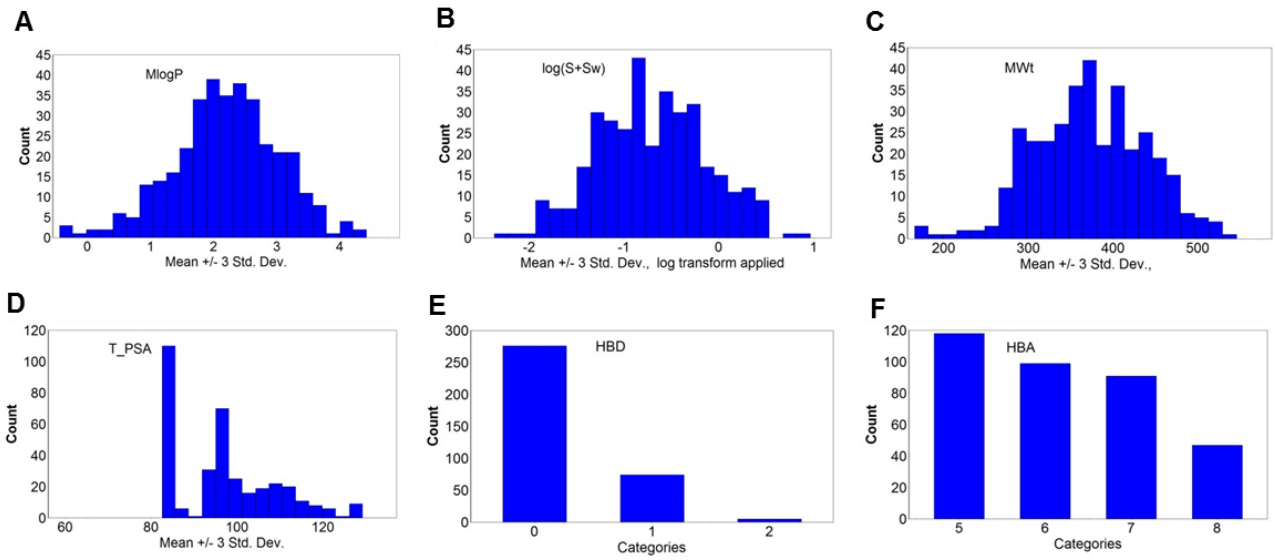

Figure S7. The property histogram of the distribution of calculated values of ADMET predictor descriptors for compounds of the pyrimidotriazinedione class: (A) Moriguchi estimation of logP, (B) logarithm of water solubility, (C) molecular weight, (D) topological version of polar surface area, (E) number of hydrogen bond donors, and (F) number of hydrogen bond acceptors.

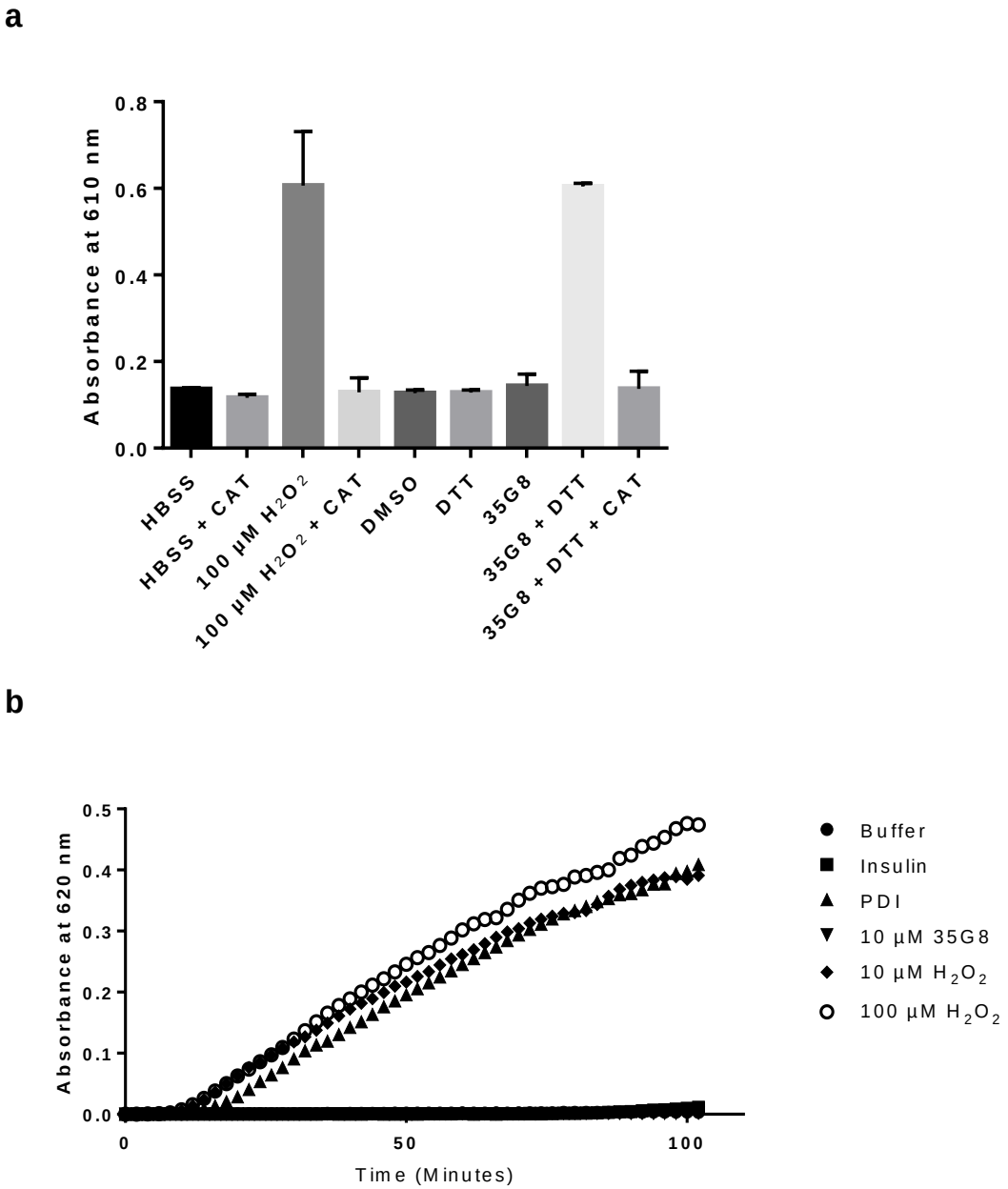

Figure S8. Redox-cycling characterstics of **35G8** do not interfere with PDI activity in the insulin turbidity assay. (A) Redox cycling assay measuring absorbance at 610 nm. Data are presented as mean ± standard deviation of three independent experiments. (B) H_2O_2 in insulin turbidity assay. Ability of PDI to reduce insulin measured in the presence of 10 µM and 100 µM H_2O_2, and 10 µM **35G8**. ● Sodium phosphate buffer only. ■ 130 µM insulin in buffer and DTT ▲ 1 µM PDI + 130 µM insulin + DTT ▼ 10 µM **35G8** in 1 µM PDI + 130 µM insulin + DTT ◆ 10 µM H_2O_2 in 1 µM PDI + 130 µM insulin + DTT ○ 100 µM H_2O_2 in 1 µM PDI + 130 µM insulin + DTT.

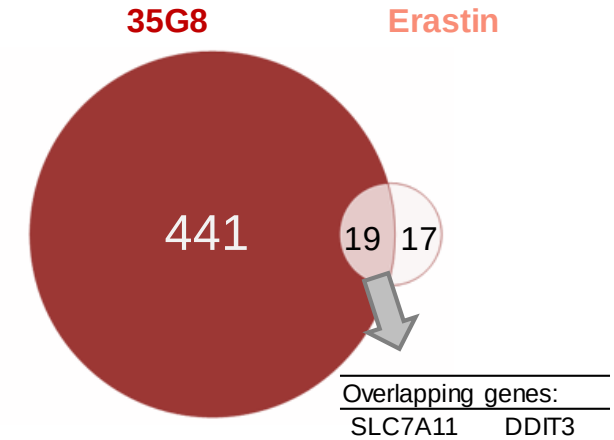

Overlapping genes:	
SLC7A11	DDIT3
CHAC1	XBP1
TRIB3	ATF3
ASNS	DDIT4
PSAT1	C9orf150
HERPUD1	CEBPG
SESN2	TUBE1
JDP2	SLC3A2
SLC7A5	GPT2
VLDLR	

Figure S9. Venn diagram comparing genes that were upregulated more than two-fold upon erastin treatment compared to DMSO treatment and genes whose rate of transcription increased upon treatment with 1 μM **35G8**.